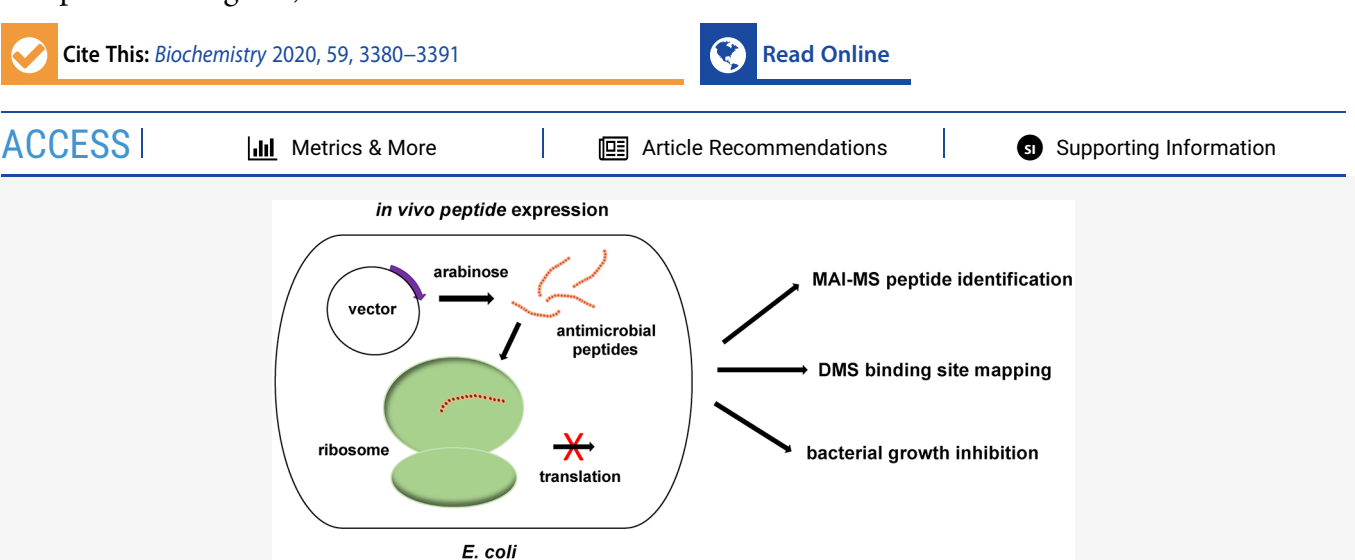
Bi@hemistry



pubs.acs.org/biochemistry Article

Expression and In Vivo Characterization of the Antimicrobial Peptide Oncocin and Variants Binding to Ribosomes

Nisansala S. Muthunayake, Rabiul Islam, Ellen D. Inutan, Wesley Colangelo, Sarah Trimpin, Philip R. Cunningham, and Christine S. Chow*



ABSTRACT: Peptides have important biomedical applications, but poor correlation between *in vitro* and *in vivo* activities can limit their development for clinical use. The ability to generate peptides and monitor their expression with new mass spectrometric methods and biological activities *in vivo* would be an advantage for the discovery and improvement of peptide-based drugs. In this study, a plasmid-based system was used to express the ribosome-targeting peptide oncocin (19 amino acids, VDKPPYLPRPRP-PRRIYNR) and to determine its direct antibacterial effects on *Escherichia coli*. Previous biochemical and structure studies showed that oncocin targets the bacterial ribosome. The oncocin peptide generated *in vivo* strongly inhibits bacterial growth. *In vivo* dimethyl sulfate footprinting of oncocin on the rRNA gives results that are consistent with those of *in vitro* studies but reveals additional binding interactions with *E. coli* ribosomes. Furthermore, expression of truncated or mutated peptides reveals which amino acids are important for antimicrobial activity. Overall, the *in vivo* peptide expression system can be used to investigate biological activities and interactions of peptides with their targets within the cellular environment and to separate contributions of the sequence to cellular transport. This strategy has future applications for improving the effectiveness of existing peptides and developing new peptide-based drugs.

The use of synthetic peptides as therapeutics has received more attention in recent years with numerous applications, including antibiotic development, 2 cancer diagnosis and treatment, 4 epitope mapping, 5 production of antibodies, 7 and vaccine design. 9 Certain characteristics of peptides such as high bioactivity, high target specificity, and low toxicity have made them attractive therapeutic agents. Furthermore, peptides are generally easier to synthesize and modify compared to natural products that require multistep syntheses or isolation. Once parent peptide sequences are identified as potential therapeutics, more potent compounds can be developed by rational design. 13–15

Antimicrobial peptides (AMPs) are examples of naturally produced compounds in bacteria, fungi, plants, and animals and play a vital role in the innate immune response. AMPs are promising candidates for further drug development. They display remarkable structural and functional diversity as well as broad spectrum activity, a low propensity to develop

bacterial resistance,²² high target specificity,²³ and strong bactericidal activity.²⁴ Incorporation of D-amino acids²⁵ and non-natural amino acids²⁶ and development of peptoids,²⁷ cyclic peptides,²⁸ and multimeric peptides²⁹ have increased the stability and expanded the range of AMP drugs. Synthetic AMPs have advantages as drug leads because they can be improved through standard methods such as position scanning with alanine, proline, or D-amino acids.^{30,31} Furthermore, a wide variety of non-natural amino acids can be employed, allowing development of large combinatorial libraries.³² Nonetheless,

Received: July 20, 2020 Revised: August 22, 2020 Published: August 25, 2020





there are still limitations in antibiotic peptide research that need to be addressed before AMPs can be applied clinically, such as the poor correlation between *in vitro* and *in vivo* activities of peptides. ^{33–35}

Determining the therapeutic potential of AMPs often begins with *in vitro* screening of synthetic peptide libraries. With such screening techniques, the crucial peptide—target interaction step occurs in a simulated environment, which is very different than an actual cellular environment. This process also requires synthesis or isolation of the target biomolecule prior to the binding experiment. After synthesis or isolation, as well as making assumptions about the physiological conditions, complex targets such as the ribosome may not be in their bioactive forms. Another concern is that targets such as RNA have numerous conformations that are influenced by their environment. Peptides are also highly sensitive to their solution conditions and can form aggregates, which may result in discrepancies between their *in vitro* and *in vivo* activities. ^{21,36,37}

Solid-phase peptide synthesis (SPPS) and peptide purification require specialized skill sets, particularly for incorporation of nonstandard amino acids. ^{33,38} After identifying an AMP from a natural source or from a peptide library screen, structural analogues are generated. The optimization process may include minimizing peptide length and systematically substituting each amino acid residue. ³⁸ This process depends on efficient amino acid couplings and suitable purification steps to remove failed sequences. ³⁸ Despite its limitations, SPPS has been highly successful in identifying a number of AMPs as potential antimicrobial agents and optimizing their biological activities. ^{39–43}

Inspired by the well-known SPPS and in vitro testing methods, we sought to develop a complementary biological approach for in-cell synthesis of ribosome-targeting peptides and study their inhibitory effects directly in bacteria. A plasmid-based system was used to express in vivo a proline-rich AMP (PrAMP) known as oncocin in Escherichia coli. Oncocin is derived from Oncopeltus fasciatus (milkweed bug), which has been optimized to be effective against Gram-negative human pathogens. 41-Previous studies showed that oncocin inhibits bacterial protein translation by targeting the ribosome. 44-46 Two groups independently identified the binding site of oncocin on the 50S subunit of Thermus thermophilus 70S ribosomes, where it blocks the peptidyl transferase center (PTC) and destabilizes the initiation complex. 47,48 Upon binding to the upper region of the peptide exit tunnel, oncocin interferes with binding of the aminoacyl-tRNA (aa-tRNA) in the A site. Although it allows formation of the initiation complex, the steric occlusion caused by the 19-amino acid (19-mer) peptide destabilizes the initiation complex and causes dissociation. 45,48 As such, oncocin inhibits protein translation by preventing the transition from initiation to

One goal of our work was to determine if *in vivo*-expressed oncocin peptides from a plasmid-based system would display bactericidal activity. The second goal was to identify the oncocin binding site within *E. coli*. An *in vivo* dimethyl sulfate (DMS) footprinting technique was employed to map peptide interactions with *E. coli* ribosomes. Several new interaction sites for oncocin were identified directly under cellular conditions, in addition to the previously reported sites in the bacterial PTC region. Furthermore, systematic amino acid replacements and truncation of the C- and N-terminal amino acid residues of the peptide revealed which residues play critical roles in the antibacterial activity of the peptide. Matrix-assisted ionization

(MAI) mass spectrometry (MS) was used to identify an expressed peptide within complex lysate compositions.

MATERIALS AND METHODS

Materials. E. coli DH5 α cells were obtained from New England Biolabs (Ipswich, MA), and plasmid vector pKan5tv-Vec is a derivative of plasmid pKan5-T1T2. 49 Plasmid isolation was performed using a QIAGEN Plasmid Maxi Kit (Germantown, MD). GoTaq Green Master Mix (2x) was purchased from Promega (Carlsbad, CA). Restriction enzymes HindIII and NheI and NEB Buffer 2.1 were obtained from New England Biolabs. Quantum Prep Freeze 'N Squeeze DNA Gel Extraction Spin Columns were acquired from Bio-Rad Laboratories (Hercules, CA). OPTIZYME T4 DNA ligase was from Fisher BioReagents (Fair Lawn, NJ). Thermo Scientific (Waltham, MA) manufactures the GeneJet Plasmid Miniprep Kit. Lysogeny broth (LB) was purchased from Sigma-Aldrich (St. Louis, MO). The polymerase chain reaction (PCR) primers to generate the inserts, universal forward and reverse primers corresponding to each peptide sequence, sequencing primers, and reverse transcription primers (5'-GCTCA ATGTT CAGTG TCAAG C-3' and 5'-GAACT GTCTC ACGAC GTTC-3') were synthesized by Integrated DNA Technologies (Coralville, IA) (Table S1). Acetonitrile and matrix-assisted ionization (MAI) matrix 3-nitrobenzonitrile (3-NBN) were purchased from Sigma-Aldrich. Zip-Tips and Amicon 10K filter columns were obtained from Millipore-Sigma (Burlington, MA).

Chemicals used in footprinting experiments, dimethyl sulfate (DMS), 2-mercaptoethanol (2-ME), sodium acetate (NaOAc), ethylenediaminetetraacetic acid (EDTA), 2-amino-2-hydroxymethylpropane-1,3-diol (Tris), phenol/chloroform/isoamyl alcohol (25:24:1, PCI), urea, acrylamide, bis(acrylamide), and isoamyl alcohol were obtained from Sigma-Aldrich or Fisher Bioreagents. Enzymes ImPromII reverse transcriptase (RT) and polynucleotide kinase (PNK) were purchased from Promega (Fitchburg, WI). [γ -32P]Adenosine 5'-triphosphate ([32 P]ATP) was obtained from PerkinElmer Life Sciences, Inc. (Waltham, MA).

Facilities and Instrumentation. Plasmid DNA samples were sequenced at the Applied Genomics Technology Center DNA Sequencing Laboratory of Wayne State University. MS analysis was carried out using MAI with a Waters SYNAPT G2S MALDI source instrument without engaging the laser. Gel images were obtained on a Typhoon 9200 with ImageQuant TL software (GE Healthcare). Optical densities (OD $_{600}$) in growth assays were measured using a Synergy H1 plate reader from Biotek (Winooski, VT).

Preparation of Vector pKan5tvVec. Vector pKan5tvVec (8243 bp) (Figure S1) has the replication setup from pACYC and selection marker (kan) from pKan5 T1T2. The Emerald GFP gene was cloned from pRSET EMGFP from Invitrogen. The TEV protease gene was cloned from pRK603 behind the EmGFP gene to make a polycistronic mRNA. Finally, the EmGFP gene was removed so that only the His tag, normalizing 5' leader peptide, TEV recognition sequence, and peptide of interest followed by a stop codon remained, which was 5' to the TEV gene. The vector DH5 α strain for pKan5tvVec was streaked from a frozen stock onto a fresh LB-agar plate with kanamycin (50 μ g/mL) and incubated overnight at 37 °C. A single colony was used to inoculate 5 mL of LB broth with kanamycin (50 μ g/mL), which was incubated for 8 h at 37 °C while being shaken (275 rpm). The 5 mL culture was added to LB broth (495 mL) with kanamycin (50 μ g/mL) and incubated

for 16 h overnight at 37 $^{\circ}$ C while being shaken (275 rpm). The culture was centrifuged (6000 rpm) at 4 $^{\circ}$ C for 15 min to obtain a cell pellet. The plasmid was isolated from the cell pellet using a QIAGEN Plasmid Maxi Kit.

Preparation of DNA Inserts with Peptide Sequences. The nontemplate PCR method was used to generate DNA inserts with the desired peptide coding sequences. The forward primer (Table S1, 10 μ L of a 5 μ M solution), reverse primer (Table S1, 10 μ L of a 5 μ M solution), GoTaq-master mixture (2×, 50 μ L), and doubly distilled H₂O (ddH₂O, 30 μ L) were combined in a 100 μ L PCR tube. The PCR mixture was heated in a thermocycler to 95 °C for 5 min to denature, then to 55 °C for 1.5 min to anneal the DNA primers, and to 72 °C for 30 s to carry out extension (30 cycles). The reaction was held at 72 °C for 7 min after the cycles were completed, and the sample was cooled to 4 °C. The PCR products were verified on 1% agarose gels (Figure S2) and purified using Quantum Prep Freeze 'N Squeeze DNA Gel Extraction Spin Columns.

The PCR product containing the desired peptide sequence (20 μ L, 1 μ g) was combined with 1 μ L of *Hin*dIII (20 units), 1 μ L of *Nhe*I (10 units), 5 μ L of NEB Buffer 2.1 (10×), and sterile ddH₂O (23 μ L). Vector pKan5tvVec (8243 bp) was digested to produce a 5371 bp fragment by combining 2.5 μ L (1 μ g) of plasmid DNA with 1 μ L of *Hin*dIII (20 units), 1 μ L of *Nhe*I (10 units), 5 μ L of NEB Buffer 2.1 (10×), and sterile ddH₂O (40.5 μ L). The reaction mixtures were incubated for 16 h at 37 °C. Quantum Prep Freeze 'N Squeeze DNA Gel Extraction Spin Columns were used to isolate the digestion fragments.

Ligation and Electrotransformation. Ligation reactions were set up for the vector (V) to insert (I) with ratios of 1:2 (V:I) with T4 DNA ligase (5 units), ligase buffer, and sterile ddH2O, and the mixtures were incubated for 1 h at room temperature and heat inactivated for 10 min at 70 °C. The ligation mixture (1.5 μ L) was added to E. coli DH5 α electrocompetent cells (25 μ L) on ice and mixed gently by pipetting. Each sample was transferred into a prechilled electroporation chamber and electroporated using an E. coli Pulser from Bio-Rad. Each sample was used to inoculate LB broth (1 mL). Cultures were incubated 37 °C for 1 h while being shaken and then transferred to microcentrifuge tubes. Cells were pelleted (5000 rpm at 4 °C for 10 min); then 800 μ L of the supernatant was removed carefully, and the pellets were resuspended in the remaining supernatant (200 μ L) and plated on prewarmed LB-agar plates with kanamycin (50 μ g/mL). Peptide clones were confirmed by colony PCR and DNA sequencing (Figure S2).

In Vivo Expression of Truncated and Amino Acid-Substituted Oncocin Variants. To generate DNA inserts for the corresponding truncated or mutated versions of the peptides, the aforementioned nontemplate PCR approach was used. The reverse primers for N-terminally truncated peptides were denoted as 18-mer reverse N (Onc Δ 1N), 17-mer reverse N (Onc Δ 2N), etc., and the reverse primers for the C-terminally truncated peptides were denoted as 18-mer reverse C (Onc Δ 1C), 17-mer reverse C (Onc Δ 2C), etc. (Table S1). The reverse primers for the alanine mutants were denoted as OncK3A, OncY6A, OncL7A, OncR11A, and OncK3AY6A-L7AR11A. Each clone of the corresponding peptide was grown to compare the growth inhibition on 3 mL of LB/kanamycin media with arabinose and without arabinose at 37 °C with a shaker speed of 250 rpm.

Characterization of the *In Vivo*-Expressed Peptide in the Cell Lysate. The DH5 α strain containing plasmid

pKanOnc (oncocin) or pKanOncΔ3N was streaked from a frozen stock on a fresh LB-agar plate with kanamycin (50 μ g/ mL) and incubated overnight at 37 °C. A single colony was used to inoculate a 3 mL culture using LB broth and kanamycin (50 $\mu g/mL$), which was incubated overnight at 37 °C while being shaken (250 rpm). From the overnight culture, 60 μ L was added to LB broth (30 mL) with kanamycin (50 μ g/mL) and incubated at 37 °C for 3–4 h until the optical density (OD₆₀₀) reached \sim 0.2. When cells reached early log phase at \sim 180 min, L-arabinose was added to a final concentration of 0.2% (w/v) to induce peptide expression. The incubation was continued for 1 h. Cells were pelleted (6000 rpm, 30 min) and then lysed by sonication. The cell lysate was centrifuged at 14000 rpm for 20 min. The supernatant was filtered through an Amicon 10K filter device to remove cellular components of >10 kDa. The flowthrough was placed under vacuum until it was dry and then redissolved in ddH_2O (50 μ L). The sample was passed through a Zip-Tip column to desalt. Mass analysis of the sample was performed using MAI-MS. Preliminary MAI-MS analysis employed the use of a pipet tip to introduce the sample. The MAI matrix, 3-NBN, was dissolved in acetonitrile (5 mg in 50 μ L). The crude, filtered, and desalted lysates (aqueous) were mixed individually with 3-NBN in a 1:1 (v/v) ratio. 50 Using a pipet tip, 1 μ L of the sample/3-NBN mixture was used, briefly dried, and exposed to the vacuum of the mass spectrometer on an overridden electrospray ionization (ESI) source on a Waters SYNAPT G2 instrument as described previously. 50 Subsequent MAI-MS analysis used the vacuum MALDI source of the Waters SYNAPT G2S instrument. 50 One microliter of the sample was placed on the metal plate with 1 μ L of a 3-NBN matrix solution using the layer method, briefly dried on the metal plate, and then introduced into the vacuum MALDI source. Ionization commenced with only 20 V on the sample metal plate and without the use of the laser, producing the typical multiply charged peptide ions of a high-resolution mass spectrometer.

Bacterial Growth Assay. Ligated plasmids containing the correct peptide coding sequences were transformed into E. coli DH5 α . Cells were grown in LB/kanamycin (50 μ g/mL) medium to prepare an overnight culture. The culture was diluted 1:500 and incubated at 37 °C for 3-4 h until the optical density (OD₆₀₀) reached \sim 0.2. When cells reached early log phase at ~180 min, L-arabinose was added to a final concentration of 0.2% (w/v) to induce expression of the peptide. Growth inhibition was carried in 25 mL of LB/ kanamycin medium with (induced) and without (uninduced) arabinose at 37 °C and 250 rpm. From each culture, 300 μ L of cells was transferred to a 96-well plate. Optical densities (OD_{600}) were measured (1:10 dilutions were found to give the same trends for growth inhibition, so nominal absorption values were used) using a Synergy H1 plate reader from Biotek every 60 min until the cells reached the stationary phase.

In Vivo DMS Footprinting. *In vivo* DMS footprinting was carried out using modified literature procedures. 51,52 The DH5α strain containing a ligated oncocin plasmid was streaked from a frozen stock onto a fresh LB-agar plate with kanamycin (50 μg/mL) and incubated overnight at 37 °C. A single colony was used to inoculate a 3 mL culture using LB broth and kanamycin (50 μg/mL), which was incubated overnight, at 37 °C while being shaken (250 rpm). From the overnight culture, $60 \mu L$ was added to LB broth (30 mL) with kanamycin (50 μg/mL) and incubated at 37 °C for 3–4 h until the optical density (OD₆₀₀) reached ~0.2. When cells reached early log phase at ~180 min, L-arabinose was added to a final concentration of 0.2% (w/v) to

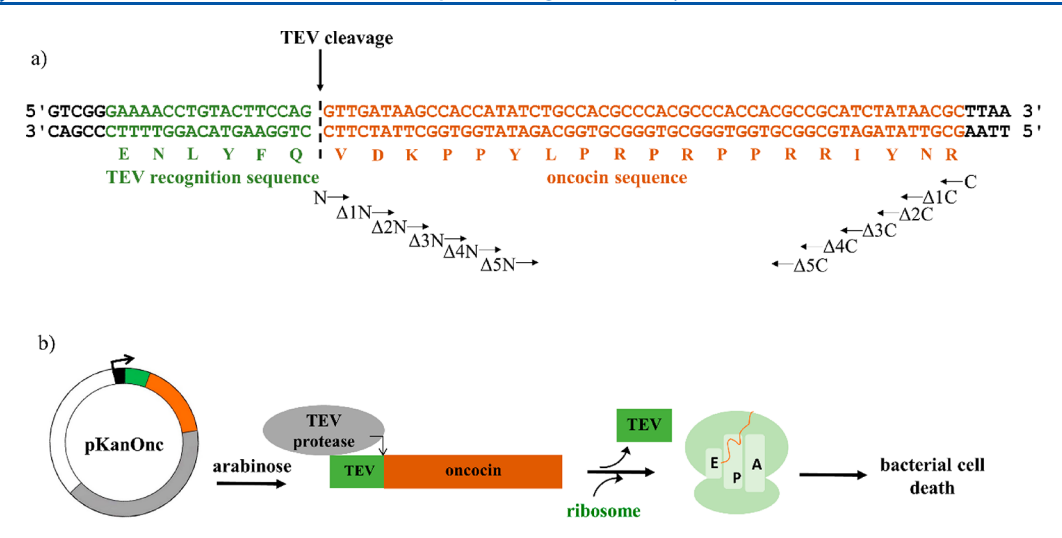


Figure 1. Schematic diagram for the production of the parent peptide oncocin and C- and N-terminal truncations. (a) The peptide coding sequences are cloned behind the TEV protease recognition sequence and under control of the P_{BAD} promoter. Truncated peptide variants are generated by systematically removing each amino acid codon from the N or C terminus of the parent peptide sequence. (b) Upon transformation of the plasmid into *E. coli* and induction with arabinose, the desired peptide precursor (pro-peptide) linked to a TEV recognition sequence on the N-terminal side and TEV protease are expressed. After TEV protease cleavage, the free peptide (e.g., oncocin) is available in the cell to bind the ribosome target and cause bacterial cell death.

induce expression of the peptide. Incubation was continued for 1 h. The probing reaction was initiated by adding 100 μ L of DMS, followed by incubation with vigorous shaking (250 rpm) for 5 min at 37 °C. The reaction was quenched by placing the tube on ice and adding 2-ME (0.6 M in ddH2O, 5 mL) and watersaturated isoamyl alcohol (5 mL). After cooling on ice for 15 min, cells were pelleted by centrifugation at 5000 rpm for 30 min at 4 °C. The upper isoamyl alcohol phase and lower aqueous phase were carefully removed from the pellet. The cell pellet was resuspended in 2-ME (0.6 M, 5 mL) and centrifuged again (5000 rpm for 30 min at 4 °C). The supernatant was carefully removed, and the cell pellet was washed with 1.5 mL of ice-cold Tris-saline buffer [10 mM Tris-HCl (pH 8), 100 mM NaCl, and 1 mM EDTA] and centrifuged again (5000 rpm, 10 min). Control experiments (no DMS, no induction with arabinose) were carried out simultaneously. The cell pellet was used for total RNA isolation using previously described methods.⁵

Reverse Transcription and Primer Extension Reactions. The extracted RNA was analyzed by using a primer extension assay with a 5'-32P-labeled DNA primer (5'-GCTCA ATGTT CAGTG TCAAG C-3') that is complementary to the peptide exit tunnel of the ribosome PTC (nucleotides G2083-C2103) and a DNA primer (5'-GAACT GTCTC ACGAC GTTC-3') that is complementary to the helix 92/helix 90 (H92/H90) region (nucleotides G2588–C2606). Gel images were obtained on a Typhoon 9200. All probing experiments were performed in triplicate (independent trials), and analyses were carried out with three experimental data sets to obtain standard errors. Band intensities were measured by using ImageQuant TL software. The background volume of an unreacted control band was subtracted from the net band volume. Then, the relative intensity was calculated by dividing the corrected target band intensity by the standard band intensity.

■ RESULTS AND DISCUSSION

Expression of the 19-mer Oncocin Peptide *In Vivo*. In this study, a plasmid-based system was used to express the ribosome-targeting peptide oncocin *in vivo* and to determine its

direct inhibitory effects on *E. coli*. The same plasmid system could then be used for *in vivo* DMS footprinting experiments to investigate binding interactions of the peptide with the ribosome within the cellular environment. In addition, the plasmid system was easily adapted to generate peptide truncations or sequence variations for *in vivo* analysis of the minimum length or sequence required for antimicrobial activity.

A single plasmid expression system, pKanStvVec (8243 bp) with an inducible P_{BAD} promoter and kanamycin resistance, was used as the starting vector (Figure S1). Primer extension PCR was used to generate the corresponding DNA sequence that encodes the desired peptide sequence. The genes were cloned behind the P_{BAD} promoter of pKanStvVec such that the peptides could be expressed by induction with L-arabinose. The peptide sequence was cloned behind the TEV (tobacco etch virus) protease recognition sequence (ENLYFQ) (Figure 1a). The coexpressed TEV protease specifically cleaves between residue Q and the N-terminal amino acid of the peptide precursor (termed pro-peptide) sequence (Figure 1b). S4,55 Therefore, after TEV protease cleavage, the N terminus of the oncocin peptide is exposed. DNA sequencing was used to confirm the cloned peptide.

Characterization of the In Vivo-Expressed Peptide in **Cell Lysates.** To confirm the presence of the expressed peptide in cell lysates, MS analysis was carried out using matrix-assisted ionization (MAI). MAI-MS using a 3-NBN matrix has been reported to ionize peptides and proteins directly out of biological materials such as tissue, whole blood, and bacteria while preferentially detecting the protonated ions. 50,56 The simple and rapid MAI approach with a pipet tip was used for preliminary MS analysis directly from cell lysate, or filtered and desalted lysate, in a mass range indicative of peptides. The desalted lysate provided qualitatively better results and was therefore used for the subsequent studies (Figure S3). By using MAI on a vacuum MALDI source of a quadrupole time-of-flight (QTOF) mass spectrometer without engaging a laser, 50,56,5 MAI-MS analysis of the desalted lysate following arabinose induction of peptide expression showed the presence of shorter peptide fragments, but not the full-length oncocin (19-mer).

The principle mass range of the prominent signals in the mass spectra was consistent with a truncated oncocin containing 16 amino acids, but no specific peptide could be unequivocally determined from the high-resolution mass spectral data. To move forward, we generated and analyzed a smaller version of oncocin, a 16-mer with removal of the three C-terminal amino acids.

The limited protease resistance of oncocin was identified as a weakness for therapeutic peptide applications. ^{58,59} More specifically, the C-terminal region of oncocin was shown to have susceptibility toward proteases, with the major site of cleavage occurring at Arg14 to generate a 14-mer peptide. ⁴¹ The protease sensitivity of oncocin can be overcome by substituting arginine with ornithine at positions 15 and 19, and the modified peptide also shows improved antibacterial activity. ⁴¹ In our studies, the MAI-MS data show that both cell lysate and desalted lysate contain a 16-mer peptide, but the high-resolution mass spectral data were not consistent with proteolytic cleavage. Examination of the mass spectra of the cell lysates did not reveal a 14-mer peptide or any low-mass m/z peaks that correspond to the loss of C-terminal amino acids.

To confirm the presence of a stable peptide in the cell extracts, a variant of oncocin with removal of the three C-terminal amino acids was cloned and expressed (16-mer, termed $Onc\Delta 3C$). The cell lysates of $Onc\Delta 3C$ were analyzed by MAI-MS. In this case, abundant ions corresponding to the truncated version of the peptide ($Onc\Delta 3C$, 16-mer) were consistently observed (Figure 2 and Figure S4). We carried out all subsequent bioactivity

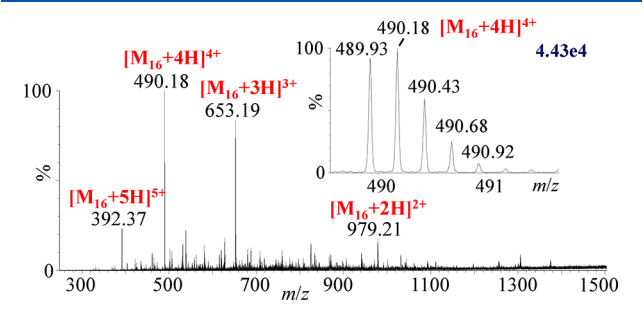


Figure 2. MAI mass spectrum of a cell lysate with the inset of the isotopic distribution of the abundant +4 charge state. The experimental monoisotopic molecular mass is calculated to be 1956.64 Da, derived from the detected +2 to +5 charge states. The theoretical monoisotopic mass of the 16-mer peptide (Onc Δ 3C) is 1956.15 Da. MAI-MS analysis used the matrix 3-NBN and was performed on a Waters SYNAPT G2S MALDI source instrument without use of the laser or instrument calibration (relative intensities are shown). 50,56,57

experiments with both full-length oncocin (19-mer) and $Onc\Delta 3C$ (16-mer), as well as other variants, for comparison. The identity of $Onc\Delta 3C$ was confirmed, but production of full-length oncocin (19-mer) and all other peptide variants was assumed going forward.

Antibacterial Activity of *In Vivo*-Expressed Peptides. Previous *in vitro* studies with chemically synthesized oncocin showed minimal inhibitory concentrations ranging from 0.125 to 8 μ g/mL for 34 different strains and clinical isolates from *E. coli, Pseudomonas aeruginosa,* and *Acinetobacter baumannii.*⁴¹ To determine the antibacterial activity of *in vivo*-expressed peptides, a bacterial growth assay was performed for oncocin and the truncated peptide Onc Δ 3C (Figure 3). Peptide expression was induced by adding arabinose at 180 min (when the OD₆₀₀ was 0.2), and bacterial growth was monitored at 60 min time

intervals (Figure 3a). After a 9 h incubation period, bacterial growth in the induced cultures is diminished by 4-fold compared to that of the uninduced controls for both oncocin and $Onc\Delta 3C$ (87% and 85% inhibition, respectively). Both peptides show 84% inhibition after a 24 h incubation period (Figure 3b).

We carried out control experiments with peptide GAAA-AAAA (Figure S5), which show 24% inhibition at 12 h following arabinose induction at 180 min. These results suggest a low level of toxicity of the expressed peptides to *E. coli*, which is not surprising given that diverting cellular resources to protein overexpression and amino acid depletion could impact cell growth. In another control experiment, substitution of the TEV recognition sequence (ENLYFQ) with AAAAAA or ENLEFQ slowed growth inhibition (38% or 66%, respectively) following arabinose induction compared to oncocin (87%) (Figure S5). The lower percentage of growth inhibition for the TEV mutants correlates with the presumed decrease in TEV activity, but the remaining inhibitory activity suggests either peptide toxicity or pro-peptide binding to ribosomes.

The similar activity of the truncated peptide (16-mer, OncΔ3C) to that of the parent oncocin (19-mer) is perhaps not surprising. Previous studies showed that the C-terminal residues are not critical for ribosome binding of oncocin but instead play a role in cell penetration. ^{45,47,48} The *in vitro* studies showed >2-fold increases in MIC values upon C-terminal truncation (e.g., 14-mer) for certain *E. coli* strains but improved activity with strains that have outer membrane defects. ⁴⁵ We note that those comparisons were done with synthetic peptides in which the parent oncocin (Onc112) has two modifications (D-arginine at positions 15 and 19) that increase its stability against proteases and improve its antimicrobial activity. ⁴⁴ Our *in vivo* results demonstrate that the plasmid-based system can be used to determine antibacterial activities of peptides and test their activity without concern for altered cell permeability.

Probing Peptide-Ribosome Interactions In Vivo. Crystal structures and in vitro probing of oncocin-bound ribosomes revealed that several 23S rRNA nucleotides in the PTC region and neighboring helices undergo changes in conformation upon peptide binding. 45,47,48 However, rRNA conformations and RNA-drug interactions could be different in a more complex cellular environment. 33,34 Therefore, we were interested in probing rRNA-oncocin interactions within the bacterial cell. We employed in vivo peptide expression combined with DMS footprinting to probe oncocin interactions with E. coli ribosomes. More specifically, changes in adenine N1 methylation by DMS can reveal oncocin interaction sites or varying conformational states due to peptide binding. Thus, alterations in the reactivities of the rRNA bases with DMS provide information about specific peptide interactions at singlenucleotide resolution. On the basis of previous in vitro probing of E. coli ribosomes and crystal structures of T. thermophilus ribosomes bound to oncocin, peptide interactions were expected to alter the DMS reactivity of nucleotides within the PTC and helix 92 (H92) region.⁴⁵

Oncocin Interacts with the PTC Region of 23S rRNA. Bacterial cells were treated with DMS 1 h after induction of oncocin expression by arabinose. Total RNA was isolated, and reverse transcription/primer extension was used to identify the N1 methylation sites of adenosine residues. The first primer was designed to probe the PTC region of 23S rRNA. Strong DMS reactivity is observed at A2058 with somewhat weaker reactivity at A2059 and A2062 (Figure 4 and Figure S6). Upon expression of oncocin, protection from DMS is observed at A2058 and

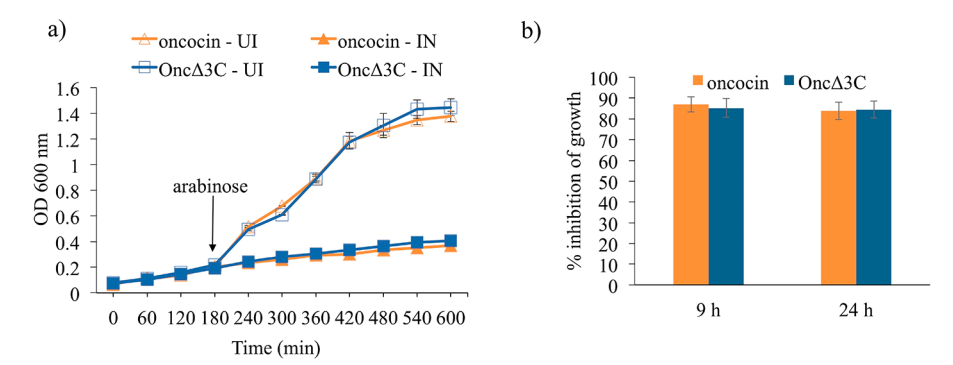


Figure 3. Growth inhibition by oncocin (19-mer) and $Onc\Delta 3C$ (16-mer) peptides. (a) Effects of the expression of oncocin and $Onc\Delta 3C$ on bacterial cell growth. Oncocin-UI (orange, empty triangles) and $Onc\Delta 3C$ -UI (blue, empty squares) are the uninduced growth curves for $DHS\alpha$ cells transformed with the pKanOnc and pKanOnc $\Delta 3C$ plasmids, whereas oncocin-IN (orange, filled triangles) and $Onc\Delta 3C$ -IN (blue, filled squares) are the corresponding samples induced with arabinose at 3 h. (b) Percent inhibition of bacterial growth after 540 min (9 h) (left) and 24 h (right) upon expression of different peptides (oncocin, orange; $Onc\Delta 3C$, blue) measured and normalized to the uninduced control. All growth assays were performed at least three times independently (standard error indicated).

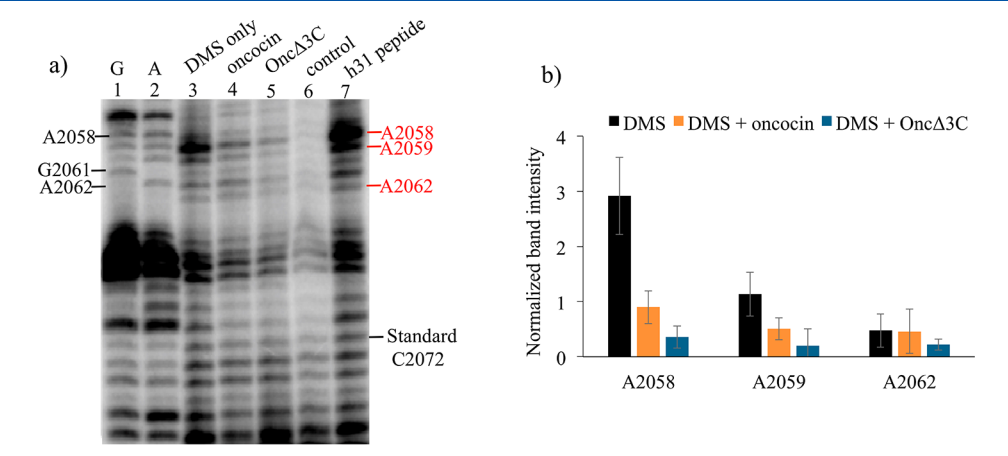


Figure 4. In vivo DMS footprinting of oncoin–PTC interactions. (a) Autoradiogram of DMS footprinting and reverse transcription/primer extension analysis at the peptide exit tunnel [lanes 1 and 2, G and A sequencing; lane 3, DMS-only control; lane 4, DMS with oncoin; lane 5, DMS with Onc Δ 3C; lane 6, no DMS control; lane 7, DMS with h31-targeting peptide (control)]. Reverse transcription stops before the DMS modification site, so the product mobility differs from the sequencing lane by one nucleotide. (b) Quantification of DMS reactivity of each nucleotide in the presence and absence of the peptide. Band intensities were normalized to a nonspecific stop site labeled as the standard at C2072. Three independent footprinting experiments were carried out (standard error indicated).

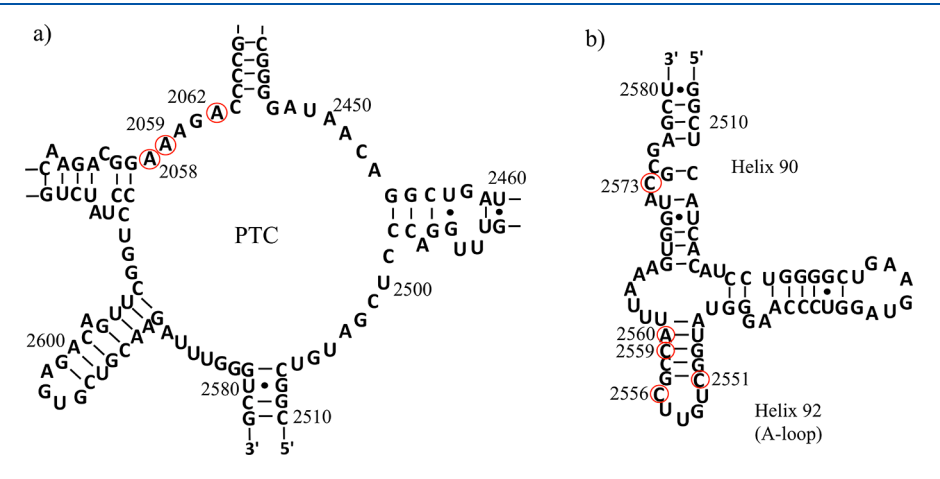


Figure 5. Summary of oncocin—rRNA interactions from DMS probing. The reactive sites identified from *in vivo* DMS footprinting experiments with *E. coli* ribosomes are circled in red on the secondary structure map⁶³ of (a) the PTC region and (b) the helix 90/helix 92 (A loop) region of 23S rRNA.

A2059 (3- and 2-fold decrease in DMS reactivity, respectively). Expression of the truncated peptide (Onc Δ 3C) also leads to reduced DMS reactivity at A2058 and A2059 (8- and 5-fold changes, respectively) relative to the control, providing support

that the C-terminal residues are not critical for ribosome binding. The differences in the DMS footprints for oncocin and the truncated peptide would suggest different binding modes or affinities. In contrast, expression of a peptide that was selected to

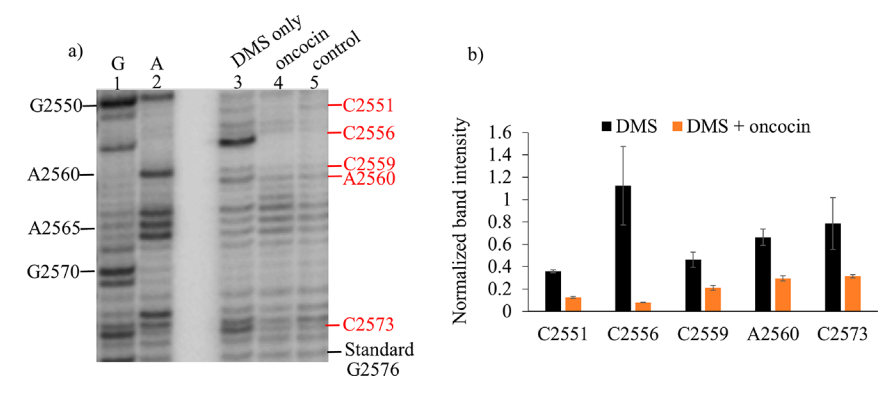


Figure 6. *In vivo* DMS footprinting of oncocin—H92 and —H90 interactions in *E. coli* ribosomes. (a) Autoradiogram of DMS footprinting and reverse transcription/primer extension analysis at helix H92 (H92, also known as the A loop): lanes 1 and 2, G and A sequencing; lane 3, DMS-only control; lane 4, DMS with oncocin; lane 5, no DMS control. (b) Quantification of DMS reactivity of each nucleotide in the presence and absence of oncocin. Band intensities were normalized to a nonspecific stop site labeled as the standard at G2576. Three independent footprinting experiments were carried out (standard error indicated).

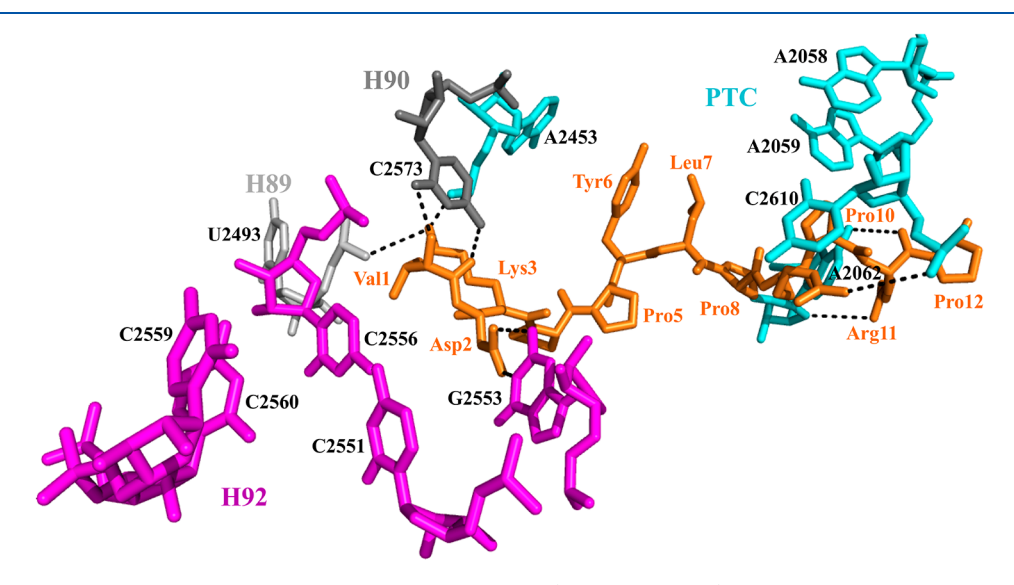


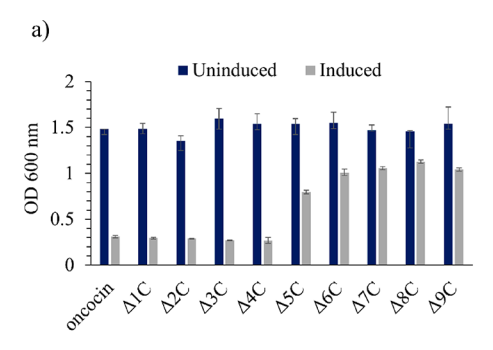
Figure 7. Interactions of oncocin with 23S rRNA. The interacting nucleotides (*E. coli* numbering) in a crystal structure of *T. thermophilus* ribosomes bound to synthetic oncocin, Onc112, are shown (PDB entry 5HCR).⁴⁵ The nucleotides from the PTC, helix 92 (H92), helix 90 (H90), and helix 89 (H89) regions are colored cyan, magenta, gray, and light gray, respectively. Residues 1–12 of Onc112 are colored orange. In the peptide exit tunnel, Arg9 and Arg11 form a stacking interaction with the nucleobases of C2610 and A2062, respectively. On the opposite end, the side chain of Asp2 forms two H-bonding interactions with G2553, a residue located in the A-loop region (H92), and the backbone of Val1 interacts with C2573 of H90. Note that residue 2560 is an A in *E. coli* and a C in *T. thermophilus*.

bind to helix 31 (h31) of 16S rRNA did not cause a decrease in DMS reactivity. The oncocin probing results are summarized on a secondary structure map of the PTC region of *E. coli* 23S rRNA (Figure 5a). The nucleotides in the upper chamber of the PTC that contact oncocin and/or undergo conformational changes upon peptide binding are highlighted (circled).

Oncocin Interacts with the A-Loop Region of 23S rRNA. We probed the interactions of oncocin with helix 92 (H92), which forms the A-loop region of 23S rRNA. Several nucleotides in the H92 region have different *in vivo* DMS reactivities upon oncocin expression (Figure 6 and Figure 87). Compared to the DMS-only control, 14-fold reduced DMS reactivity is observed at residue C2556 in the loop region. Residues C2551, C2559, and A2560 in the stem region of H92 are also protected from DMS modification by oncocin (3-, 2-, and 2-fold reduced reactivity, respectively). Residue C2573 in the stem region of helix 90 (H90) also shows 2.5-fold reduced DMS reactivity. The oncocin probing results are summarized on a secondary structure map of the H90 and H92 region of *E. coli*

23S rRNA (Figure 5b).⁶³ The nucleotides that contact oncocin and/or undergo conformational changes upon peptide binding are highlighted (circled).

Comparison of In Vivo Probing Results with Crystal **Structures.** In crystal structures of an oncocin peptide bound to T. thermophilus ribosomes, nucleotide A2062 of 23S rRNA adopts a conformation that allows the base to form a favorable stacking interaction with Arg11 of the peptide (Figure 7).^{47,48} Furthermore, it has been shown that substitution of Arg11 with alanine decreases the affinity of oncocin for *E. coli* ribosomes by 6-fold. 44 However, our *in vivo* footprinting data do not reveal any change in DMS reactivity at A2062 when oncocin is expressed compared to the DMS-only control (Figure 4), which agree qualitatively with the results of previous in vitro footprinting experiments with a synthetic oncocin variant, Onc112.45 In in vitro footprinting experiments, the presence of Onc112 did not impact the DMS reactivity of A2062, but Bac7 (a related PrAMP) showed enhanced DMS reactivity at A2062.⁴⁵ Our in vivo results do not rule out a direct A2062—oncocin interaction.



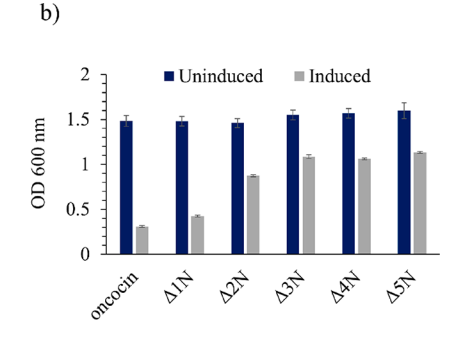


Figure 8. Role of N- and C-terminal residues of oncocin in antibacterial activity. The effects of the *in vivo* expression of (a) C-terminally and (b) N-terminally truncated peptides on bacterial cell growth are summarized, with a comparison of uninduced (blue bars) and induced (arabinose-treated, gray bars, 6 h after induction) samples. All growth assays were performed at least three times independently (standard error indicated).

Conformational changes caused by oncocin—A2062 interactions may not be large enough to alter the reactivity of this adenine residue toward DMS, or this residue has limited solvent exposure in the unbound state.

Reduced band intensities at the reverse transcription stop sites corresponding to A2058 and A2059 (DMS-treated) compared to the DMS-only control indicate protection of these nucleotides by in vivo-expressed oncocin (E. coli) (Figures 4 and 5). Even greater protection of those residues by the 16-mer peptide (Onc Δ 3C) compared to that of oncocin suggests tighter binding by the smaller peptide, or an enhanced conformational change that increases the degree of solvent exposure of those nucleotides. In contrast to the observations with A2062, crystal structures of T. thermophilus ribosomes did not reveal any direct interactions between oncocin and A2058 or A2059, and in vitro DMS probing with E. coli ribosomes did not show any changes in reactivity at those residues.⁴⁵ However, these two nucleotides are recognized as the main constituents of the macrolide (e.g., azithromycin and erythromycin) binding pocket within the PTC region (Figure S8), with a key role in binding selectivity.⁶⁴⁻⁶⁷ Previous in vitro footprinting with erythromycin showed strong DMS protection of A2058 and A2059 in ribosomes from archaea (Halobacterium halobium) and three different bacterial species (Deinococcus radiodurans, E. coli, or Staphylococcus aureus).67 Thus, our in vivo results suggest that the oncocin peptide and OncΔ3C have some overlap with the macrolide binding site.

The intrinsic dynamics of the ribosome and peptide in solution, especially within a more complex cellular environment, could lead to alternative binding modes and thus different exposures to DMS.⁶⁸ We note that only truncated versions of oncocin (12-mer or 13-mer) were observed in the crystal structures and the first 8–10 amino acids were modeled; therefore, these structures do not account for additional interactions that might occur with longer variants of the peptide such as a 16-mer or a 19-mer.^{47,48} Also of note is the fact that residue 2560 in H92 is a C in *T. thermophilus* ribosomes and an A in *E. coli* ribosomes, which could also impact the rRNA structure, particularly at the neighboring C2556, as well as interactions with oncocin (Figure 7).

Reduced band intensities at C2573, C2551, C2556, C2559, and A2560 (DMS-treated) compared to those of the DMS-only control indicate protection of these nucleotides by *in vivo*-expressed oncocin (*E. coli*) (Figures 5b and 6). Crystal structures of *T. thermophilus* ribosomes with Onc112 (Figure 7 and Figure S9) revealed that the first three amino acids of oncocin (VDK) participate in multiple interactions with these

H90 and H92 residues. 45,47,48 Residues C2573 and G2553 form hydrogen bonds with the Val1 backbone and side chain of Asp2, respectively. 45,64 Thus, altered DMS reactivity at these sites is consistent with direct oncocin interactions. Changes in DMS reactivity also occur at C2556, which is located near G2553. It is noteworthy that nucleotide G2553 is part of the A loop and forms a Watson-Crick pair with C75 of the aa-tRNA.⁶⁹ Residues C2573 and C2556, together with G2553, are part of the aa-tRNA accommodation gate and therefore play an important role in translation. ⁷⁰ As such, interactions of oncocin with H90 and H92 could interfere with binding of the CCA end of aa-tRNA and inhibit the transition of the ribosome from the initiation to the elongation phase. Previous studies also showed that mutations at C2573 lead to impaired RF2-catalyzed peptide release, highlighting the important role of this residue with respect to ribosome function and antibiotic targeting.⁷¹ Our in vivo DMS probing of the interactions of the PTC, H90, and H92 nucleotides with oncocin provides insight into the peptideribosome interactions under cellular conditions and provides further evidence for the mechanism of action of oncocin with respect to interference with binding of aa-tRNA to the PTC region.45,48

Roles of Oncocin Residues in Antibacterial Activity. To examine the functional length of oncocin, we systematically truncated one amino acid at a time from the N or C terminus of oncocin (Figure 1a). Truncated peptides were cloned and expressed in E. coli, and bacterial growth in the presence or absence of arabinose was monitored. Our data reveal that removal of the four C-terminal amino acids of oncocin does not affect antibacterial activity. The C-terminally truncated peptides, Onc Δ 1C, Onc Δ 2C, Onc Δ 3C, and Onc Δ 4C, retain antibacterial activities similar to that of full-length oncocin (Figure 8a). Removal of the fifth C-terminal amino acid (Onc Δ 5C) leads to 2.5-fold reduced activity compared to that of the 19-mer oncocin. In contrast, a >3-fold reduction in antibacterial activity is observed upon deletion of six or more amino acids from the C terminus (Figure 8a). These data suggest that the last four Cterminal amino acids of oncocin are not critical for its antibacterial activity.

In contrast to the C-terminal truncation results, N-terminal deletions lead to a significant reduction in antibacterial activity (Figure 8b). A sequential decrease in antibacterial activity is observed upon deletion of each amino acid from the N terminus. The truncated peptides $\text{Onc}\Delta 1\text{N}$, $\text{Onc}\Delta 2\text{N}$, $\text{Onc}\Delta 3\text{N}$, $\text{Onc}\Delta 4\text{N}$, and $\text{Onc}\Delta 5\text{N}$ show 1.4-, 3-, 3.5-, 3.5-, and 4-fold decreased antibacterial activity, respectively, compared to that of the parent peptide oncocin (Figure 8b). These data show the

importance of the N-terminal residues for the antibacterial activity of oncocin, consistent with previous work with synthetic peptides that showed ≥ 2 -fold increases in MIC values, depending on the bacterial strains. The N-terminal deletions could also impact TEV protease efficiency. Previous reports showed that certain amino acids slow the cleavage of TEV, some with complete inhibition. In particular, proline was shown in that work to inhibit TEV cleavage. However, two of the deletions (Onc $\Delta 3N$ and Onc $\Delta 4N$) have proline at the TEV cleavage site but show growth inhibition upon induction with arabinose, consistent with active TEV or possibly ribosome binding by the pro-peptide.

In ribosome crystal structures with bound oncocin, the N terminus of the peptide is oriented toward the PTC while the C terminus protrudes into the peptidyl exit tunnel (Figure 7). 45,47,48 The first three N-terminal amino acids form multiple interactions with 23S rRNA and align at the site that interacts with the CCA end of the aa-tRNA. 45,47,48 The N-terminal residues of oncocin play a key role in the ribosome stalling mechanism, whereas the C-terminal residues have been shown to play a role in cell penetration. 44,48 Our in vivo peptide truncation data suggest that the functional length of oncocin is 15 amino acid residues from the N terminus. This observation correlates qualitatively with the results of previously published in vitro studies using synthetic peptides. More specifically, results from cell-free transcription-translation assays showed that a 14mer peptide inhibits translation inhibition to the same extent as a 19-mer peptide. 45 In that same study, a toe-printing experiment revealed that the truncated and 19-mer peptides stalled ribosomes similarly.45

In Vivo Expression of Alanine Mutants of Oncocin. Our DMS probing and truncation data suggest that the N-terminal residues of oncocin are responsible for targeting the ribosome, whereas prior studies indicated that the positively charged residues distributed throughout the peptide sequence play a role in cellular uptake of the peptide. 44,45,48 In one study, a positional alanine scan was carried out and mutations K3A, Y6A, L7A, and R11A were shown to completely abolish the antibacterial activity of the 19-mer oncocin. 42 We substituted each of these amino acids in oncocin with alanine to produce four mutants (OncK3A, OncY6A, Onc7LA, and OncR11A). In addition, all four positions were substituted with alanine to obtain the OncK3AY6AL7AR11A mutant.

A summary of the antibacterial activity for the five alanine mutants compared to that of the parent peptide oncocin is shown in Figure 9. For OncK3AY6AL7AR11A, a significant loss of antibacterial activity was observed after induction for 6 h (only 6% growth inhibition). The OncK3A mutant also showed loss of antimicrobial activity, with only 18% growth inhibition compared to 80% for oncocin. In crystal structures, the aromatic side chain of Tyr6 participates in a π -stacking interaction with C2452 of 23S rRNA. 45 The backbone of Leu7 forms two hydrogen bonds with U2506. Previous mutagenesis experiments showed that alanine substitution of either residue in oncocin reduced ribosome binding affinity by a factor of 7 and resulted in a complete loss of inhibitory activity on in vitro translation.⁴⁴ Bacterial growth assays were performed with OncY6A and OncL7A, and both mutants showed a loss of antibacterial activity (20% and 21% inhibition, respectively) compared to oncocin (Figure 9). These in vivo observations show trends similar to those of previous alanine-scanning mutagenesis experiments with oncocin in which substitution at Tyr6 or Leu7 led to a 32-fold increase in MIC values against E. coli. 42

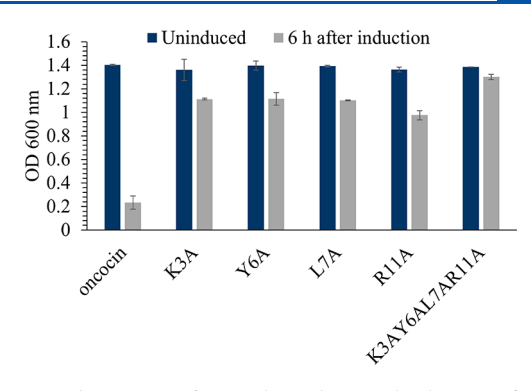


Figure 9. Substitution of critical residues with alanine affects the antibacterial activity of oncocin. The effects of the *in vivo* expression of alanine mutants on bacterial cell growth are summarized, with a comparison of uninduced (blue bars) and induced (arabinose-treated, gray bars, 6 h time points) samples. All growth assays were performed at least three times independently (standard error indicated).

Crystal structures also revealed that the C-terminal PRPRP motif of oncocin interacts with 23S rRNA, including π -stacking interactions between the guanidino groups of Arg9 and Arg11 and nucleotides C2610 and A2062. ^{45,47,48} Previous mutagenesis experiments showed that substitution of Arg11 with alanine in oncocin (or synthetic derivatives) reduced the ribosome binding affinity by a factor of 6 and increased the MIC value of the peptide by 8–16-fold. ^{42,44} In growth assays, a loss of antibacterial activity was observed with OncR11A, with 28% inhibition after incubation for 6 h.

In our alanine-substitution experiments, four residues, Lys3, Tyr6, Leu7, and Arg11, are shown to be important for the antibacterial activity of oncocin; however, we cannot rule out the possibility that the mutant peptides could be more susceptible to protease degradation *in vivo*. Nonetheless, the *in vivo* expression and growth inhibition data suggest that optimization processes for AMPs (such as alanine scanning) could be carried out with the plasmid-based system to complement SPPS and MIC, ribosome binding, and translation—inhibition studies. At later stages of optimization, the *in vivo* assay could be used in combination with SPPS and DMS mapping on the ribosome to obtain more information about the antibacterial activity of selected peptide variants. Similarly, mutants could be further chemically modified with non-natural amino acids by SPPS following sequence optimization *in vivo*.

CONCLUSIONS

In this study, a plasmid-based approach was utilized to express in vivo a peptide antibiotic, oncocin, as well as alanine mutants and C- and N-terminally truncated versions of the parent peptide. Despite the availability of crystal structures of AMPs bound to ribosomes, some details may not be revealed, such as dynamics under solution conditions of a cell, secondary binding sites, or the ability to correlate binding directly with biological activity. The *in vivo* expression of oncocin can be coupled with growth assays to determine the antibacterial activity and footprinting experiments to reveal which rRNA nucleotides undergo changes in exposure to chemical probes upon peptide binding. Under in vivo conditions, DMS probing revealed binding of oncocin in the PTC region as well as the macrolide binding pocket. Analysis of the cell lysates provides information about peptide expression and cellular stability. In this study, MAI-MS was highly useful for quickly and reliably analyzing lysates for the presence of peptides

in a complex mixture, requiring only several measurements and small sample amounts (1 μ L of cell lysate).

Because the plasmid-based system allows for the production of peptides inside bacterial cells, there are additional applications of this technology, such as screening peptide libraries. Past studies employed oncocin-based peptide libraries to identify analogues with improved antibacterial activity against Gram-positive bacterial strains. 73 These studies were entirely dependent on SPPS. Some limitations of SPPS include the low reactivity of secondary amines, making the synthesis and purification of proline-rich peptides particularly challenging without the proper expertise. The in vivo peptide expression approach has some advantages over SPPS for generation of PrAMP-based libraries, while allowing the antibacterial activities and mechanism of action to be assessed simultaneously. The SPPS and bacterial expression approaches are therefore complementary with each having strengths that can ultimately lead to successful peptide-based antimicrobial drugs.

The in vivo expression and in vivo DMS footprinting provide information about peptide-ribosome interactions within the cellular environment. Such information is useful for future antibiotic drug development with specific targeting of the rRNA. This method is not limited to PrAMPs, however, and could be expanded to explore a wide variety of other peptide drug candidates. Similarly, DMS probing has been used to analyze the structures of small RNAs and RNA-protein complexes (RNPs),74 and in vivo DMS probing has been used to gain information about bacterial and eukaryotic ribosome biogenesis.⁷⁵ Coupling of DMS probing with high-throughput sequencing could be used to greatly increase the level of information about the RNA targets and drug interactions. 76,77 Therefore, future work could involve in vivo peptide expression, growth assays, and DMS probing and complete RNA sequencing to determine the binding sites as well as secondary sites.

For future applications to be successful, in vivo peptide selections would need to be combined with SPPS such that after sequences are optimized for activity and cell lysates examined for peptide stability, non-natural amino acids [e.g., α -amino-3guanidino-propionic acid, homoarginine, nitro-arginine, Nmethyl-arginine, β -homoarginine, D-arginine, or ornithine (Orn)] could be incorporated at the major proteolytic sites, which was done previously with AMPs. 43 Another consideration is that the in vivo expression technology can be used as a rapid screening tool but provides only relative information about bacterial growth. There could be false negatives if the TEV protease efficiency is impacted by mutations (especially at the N-terminal position of the peptide)⁷² or if translational efficiency is impacted by the mutation. The peptide could also inhibit its own production and possible TEV production, so all hits need to be verified by in vitro methods with synthetic peptides. Nonetheless, the combined in vivo expression and MAI-MS approach still has many advantages with potential uses in future drug discovery and PrAMP optimization.

ASSOCIATED CONTENT

Supporting Information

The Supporting Information is available free of charge at https://pubs.acs.org/doi/10.1021/acs.biochem.0c00600.

Additional information (PDF)

AUTHOR INFORMATION

Corresponding Author

Christine S. Chow — Department of Chemistry, Wayne State University, Detroit, Michigan 48202, United States; orcid.org/0000-0002-5538-4553; Email: cchow@wayne.edu

Authors

Nisansala S. Muthunayake — Department of Chemistry and Department of Biological Sciences, Wayne State University, Detroit, Michigan 48202, United States

Rabiul Islam – Department of Chemistry, Wayne State University, Detroit, Michigan 48202, United States

Ellen D. Inutan – Department of Chemistry, Mindanao State University-Iligan Institute of Technology, Iligan 9200, Philippines

Wesley Colangelo — Department of Biological Sciences, Wayne State University, Detroit, Michigan 48202, United States

Sarah Trimpin – Department of Chemistry, Wayne State University, Detroit, Michigan 48202, United States

Philip R. Cunningham – Department of Biological Sciences, Wayne State University, Detroit, Michigan 48202, United States

Complete contact information is available at: https://pubs.acs.org/10.1021/acs.biochem.0c00600

Funding

The authors are grateful for the generous support from NSF STTR Phase II 1556043 including TECP and NSF SBIR Phase I 1913787 (to S.T.).

Notes

The authors declare no competing financial interest.

ACKNOWLEDGMENTS

The authors thank Prabuddha Waduge for cloning the h31 control peptide and the Lumigen Instrument Center for technical support.

ABBREVIATIONS

AMP, antimicrobial peptide; DMS, dimethyl sulfate; ESI, electrospray ionization; h31, helix 31; H90, helix 90; H92, helix 92; MAI, matrix-assisted ionization; MALDI, matrix-assisted laser desorption ionization; 2-ME, 2-mercaptoethanol; MIC, minimum inhibitory concentration; MS, mass spectrometry; 3-NBN, 3-nitrobenzonitrile; PCI, phenol/chloroform/isoamyl alcohol; PNK, polynucleotide kinase; PrAMP, prolinerich antimicrobial peptide; PTC, peptidyl transferase center; QTOF, quadrupole time-of-flight; RT, reverse transcriptase; TEV, tobacco etch virus; TOF, time-of-flight; SPPS, solid-phase peptide synthesis.

REFERENCES

- (1) Pizzolato-Cezar, L. R., Okuda-Shinagawa, N. M., and Machini, M. T. (2019) Combinatory therapy antimicrobial peptide-antibiotic to minimize the ongoing rise of resistance. *Front. Microbiol.* 10, 1703–1707.
- (2) Lei, J., Sun, L., Huang, S., Zhu, C., Li, P., He, J., Mackey, V., Coy, D. H., and He, Q. (2019) The antimicrobial peptides and their potential clinical applications. *Am. J. Transl. Res.* 11, 3919–3931.
- (3) Yavari, B., Mahjub, R., Saidijam, M., Raigani, M., and Soleimani, M. (2018) The potential use of peptides in cancer treatment. *Curr. Protein Pept. Sci.* 19, 759–770.
- (4) Xiao, Y.-F., Jie, M.-M., Li, B.-S., Hu, C.-J., Xie, R., Tang, B., and Yang, S.-M. (2015) Peptide-based treatment: a promising cancer therapy. *J. Immunol. Res.* 2015, 761820–761832.

- (5) Li Pira, G., Ivaldi, F., Moretti, P., and Manca, F. (2010) High throughput T epitope mapping and vaccine development. *J. Biomed. Biotechnol.* 2010, 325720—325757.
- (6) Irving, M. B., Pan, O., and Scott, J. K. (2001) Random-peptide libraries and antigen-fragment libraries for epitope mapping and the development of vaccines and diagnostics. *Curr. Opin. Chem. Biol. 5*, 314–324.
- (7) Lee, B.-S., Huang, J.-S., Jayathilaka, L. P., Lee, J., and Gupta, S. (2016) Antibody production with synthetic peptides. *Methods Mol. Biol.* 1474, 25–47.
- (8) Trier, N., Hansen, P., and Houen, G. (2019) Peptides, antibodies, peptide antibodies and more. *Int. J. Mol. Sci.* 20, 6289–6310.
- (9) Skwarczynski, M., and Toth, I. (2016) Peptide-based synthetic vaccines. Chem. Sci. 7, 842-854.
- (10) Tam, J. P. (1988) Synthetic peptide vaccine design: synthesis and properties of a high-density multiple antigenic peptide system. *Proc. Natl. Acad. Sci. U. S. A. 85*, 5409–5413.
- (11) Lau, J. L., and Dunn, M. K. (2018) Therapeutic peptides: historical perspectives, current development trends, and future directions. *Bioorg. Med. Chem.* 26, 2700–2707.
- (12) Lee, A. C.-L., Harris, J. L., Khanna, K. K., and Hong, J.-H. (2019) A comprehensive review on current advances in peptide drug development and design. *Int. J. Mol. Sci.* 20, 2383–2403.
- (13) Ghosh, C., and Haldar, J. (2015) Membrane-active small molecules: designs inspired by antimicrobial peptides. *ChemMedChem* 10, 1606–1624.
- (14) Fosgerau, K., and Hoffmann, T. (2015) Peptide therapeutics: current status and future directions. *Drug Discovery Today* 20, 122–128.
- (15) Yang, Z., He, S., Wang, J., Yang, Y., Zhang, L., Li, Y., and Shan, A. (2019) Rational design of short peptide variants by using kunitzin-RE, an amphibian-derived bioactivity peptide, for acquired potent broad-spectrum antimicrobial and improved therapeutic potential of commensalism coinfection of pathogens. J. Med. Chem. 62, 4586–4605.
- (16) Maróti, G., Kereszt, A., Kondorosi, E., and Mergaert, P. (2011) Natural roles of antimicrobial peptides in microbes, plants and animals. *Res. Microbiol.* 162, 363–374.
- (17) Zhang, L.-J., and Gallo, R. L. (2016) Antimicrobial peptides. Curr. Biol. 26, R14–R19.
- (18) Ganz, T. (2003) The role of antimicrobial peptides in innate immunity. *Integr. Comp. Biol.* 43, 300–304.
- (19) Pasupuleti, M., Schmidtchen, A., and Malmsten, M. (2012) Antimicrobial peptides: key components of the innate immune system. *Crit. Rev. Biotechnol.* 32, 143–171.
- (20) Hancock, R. E. (2001) Cationic peptides: effectors in innate immunity and novel antimicrobials. *Lancet Infect. Dis.* 1, 156–164.
- (21) Mahlapuu, M., Håkansson, J., Ringstad, L., and Björn, C. (2016) Antimicrobial peptides: an emerging category of therapeutic agents. *Front. Cell. Infect. Microbiol.* 6, 194–205.
- (22) Andersson, D. I., Hughes, D., and Kubicek-Sutherland, J. Z. (2016) Mechanisms and consequences of bacterial resistance to antimicrobial peptides. *Drug Resist. Updates* 26, 43–57.
- (23) Xu, L., Shao, C., Li, G., Shan, A., Chou, S., Wang, J., Ma, Q., and Dong, N. (2020) Conversion of broad-spectrum antimicrobial peptides into species-specific antimicrobials capable of precisely targeting pathogenic bacteria. *Sci. Rep. 10*, 944–952.
- (24) Lehrer, R. I., Barton, A., Daher, K. A., Harwig, S. S., Ganz, T., and Selsted, M. E. (1989) Interaction of human defensins with Escherichia coli. Mechanism of bactericidal activity. *J. Clin. Invest.* 84, 553–561.
- (25) Di Grazia, A., Cappiello, F., Cohen, H., Casciaro, B., Luca, V., Pini, A., Di, Y. P., Shai, Y., and Mangoni, M. L. (2015) D-Amino acids incorporation in the frog skin-derived peptide esculentin-1a(1–21)NH2 is beneficial for its multiple functions. *Amino Acids* 47, 2505–2519.
- (26) Oliva, R., Chino, M., Pane, K., Pistorio, V., De Santis, A., Pizzo, E., D'Errico, G., Pavone, V., Lombardi, A., Del Vecchio, P., Notomista, E., Nastri, F., and Petraccone, L. (2018) Exploring the role of unnatural amino acids in antimicrobial peptides. *Sci. Rep. 8*, 8888–8903.

- (27) Hooks, J. C., Matharage, J. P., and Udugamasooriya, D. G. (2011) Development of homomultimers and heteromultimers of lung cancerspecific peptoids. *Biopolymers* 96, 567–577.
- (28) Russo, A., Aiello, C., Grieco, P., and Marasco, D. (2016) Targeting "undruggable" proteins: design of synthetic cyclopeptides. *Curr. Med. Chem.* 23, 748–762.
- (29) Giuliani, A., and Rinaldi, A. C. (2011) Beyond natural antimicrobial peptides: multimeric peptides and other peptidomimetic approaches. *Cell. Mol. Life Sci.* 68, 2255–2266.
- (30) Herning, T., Yutani, K., Inaka, K., Kuroki, R., Matsushima, M., and Kikuchi, M. (1992) Role of proline residues in human lysozyme stability: a scanning calorimetric study combined with X-ray structure analysis of proline mutants. *Biochemistry* 31, 7077–7085.
- (31) Peeters, T. L., Macielag, M. J., Depoortere, I., Konteatis, Z. D., Florance, J. R., Lessor, R. A., and Galdes, A. (1992) D-amino acid and alanine scans of the bioactive portion of porcine motilin. *Peptides 13*, 1103–1107.
- (32) Astle, J. M., Simpson, L. S., Huang, Y., Reddy, M. M., Wilson, R., Connell, S., Wilson, J., and Kodadek, T. (2010) Seamless bead to microarray screening: rapid identification of the highest affinity protein ligands from large combinatorial libraries. *Chem. Biol.* 17, 38–45.
- (33) Wimley, W. C., and Hristova, K. (2011) Antimicrobial peptides: successes, challenges and unanswered questions. *J. Membr. Biol.* 239, 27–34.
- (34) Mandal, S. M., Roy, A., Ghosh, A. K., Hazra, T. K., Basak, A., and Franco, O. L. (2014) Challenges and future prospects of antibiotic therapy: from peptides to phages utilization. *Front. Pharmacol. 5*, 105–116.
- (35) Guilhelmelli, F., Vilela, N., Albuquerque, P., da S. Derengowski, L., Silva-Pereira, I., and Kyaw, C. M. (2013) Antibiotic development challenges: the various mechanisms of action of antimicrobial peptides and of bacterial resistance. *Front. Microbiol.* 4, 353–364.
- (36) Hsu, C.-H., Chen, C., Jou, M.-L., Lee, A. Y., Lin, Y.-C., Yu, Y.-P., Huang, W.-T., and Wu, S.-H. (2005) Structural and DNA-binding studies on the bovine antimicrobial peptide, indolicidin: evidence for multiple conformations involved in binding to membranes and DNA. *Nucleic Acids Res.* 33, 4053–4064.
- (37) Jenssen, H., Hamill, P., and Hancock, R. E. W. (2006) Peptide antimicrobial agents. Clin. Microbiol. Rev. 19, 491–511.
- (38) Bray, B. L. (2003) Large-scale manufacture of peptide therapeutics by chemical synthesis. *Nat. Rev. Drug Discovery* 2, 587–503
- (39) Li, W., Tailhades, J., O'Brien-Simpson, N. M., Separovic, F., Otvos, L., Jr., Hossain, M. A., and Wade, J. D. (2014) Proline-rich antimicrobial peptides: potential therapeutics against antibiotic-resistant bacteria. *Amino Acids* 46, 2287–2294.
- (40) Mishra, A. K., Choi, J., Moon, E., and Baek, K.-H. (2018) Tryptophan-rich and proline-rich antimicrobial peptides. *Molecules* 23, 815–838.
- (41) Knappe, D., Piantavigna, S., Hansen, A., Mechler, A., Binas, A., Nolte, O., Martin, L. L., and Hoffmann, R. (2010) Oncocin (VDKPPYLPRPRPPRRIYNR-NH2): a novel antibacterial peptide optimized against gram-negative human pathogens. *J. Med. Chem.* 53, 5240–5247.
- (42) Knappe, D., Zahn, M., Sauer, U., Schiffer, G., Sträter, N., and Hoffmann, R. (2011) Rational design of oncocin derivatives with superior protease stabilities and antibacterial activities based on the high-resolution structure of the oncocin-DnaK complex. *ChemBioChem* 12, 874–876.
- (43) Knappe, D., Kabankov, N., and Hoffmann, R. (2011) Bactericidal oncocin derivatives with superior serum stabilities. *Int. J. Antimicrob. Agents* 37, 166–170.
- (44) Krizsan, A., Volke, D., Weinert, S., Sträter, N., Knappe, D., and Hoffmann, R. (2014) Insect-derived proline-rich antimicrobial peptides kill bacteria by inhibiting bacterial protein translation at the 70S ribosome. *Angew. Chem., Int. Ed.* 53, 12236–12239.
- (45) Gagnon, M. G., Roy, R. N., Lomakin, I. B., Florin, T., Mankin, A. S., and Steitz, T. A. (2016) Structures of proline-rich peptides bound to

- the ribosome reveal a common mechanism of protein synthesis inhibition. *Nucleic Acids Res.* 44, 2439–2450.
- (46) Krizsan, A., Prahl, C., Goldbach, T., Knappe, D., and Hoffmann, R. (2015) Short proline-rich antimicrobial peptides inhibit either the bacterial 70S ribosome or the assembly of its large 50S subunit. *ChemBioChem 16*, 2304–2308.
- (47) Roy, R. N., Lomakin, I. B., Gagnon, M. G., and Steitz, T. A. (2015) The mechanism of inhibition of protein synthesis by the proline-rich peptide oncocin. *Nat. Struct. Mol. Biol.* 22, 466–469.
- (48) Seefeldt, A. C., Nguyen, F., Antunes, S., Pérébaskine, N., Graf, M., Arenz, S., Inampudi, K. K., Douat, C., Guichard, G., Wilson, D. N., and Innis, C. A. (2015) The proline-rich antimicrobial peptide Onc112 inhibits translation by blocking and destabilizing the initiation complex. *Nat. Struct. Mol. Biol.* 22, 470–475.
- (49) Colangelo, W. D. (2012) In vivo display: a selection and its derivatives for antimicrobial peptide lead identification. Ph.D. Dissertation, Wayne State University, Detroit.
- (50) Inutan, E. D., and Trimpin, S. (2013) Matrix assisted ionization vacuum (MAIV), a new ionization method for biological materials analysis using mass spectrometry. *Mol. Cell. Proteomics* 12, 792–796.
- (51) Waduge, P., Sakakibara, Y., and Chow, C. S. (2019) Chemical probing for examining the structure of modified RNAs and ligand binding to RNA. *Methods* 156, 110–120.
- (52) Wells, S. E., Hughes, J. M., Haller Igel, A., and Ares, M., Jr. (2000) Use of dimethyl sulfate to probe RNA structure in vivo. *Methods Enzymol.* 318, 479–493.
- (53) Ban, N., Nissen, P., Hansen, J., Moore, P. B., and Steitz, T. A. (2000) The complete atomic structure of the large ribosomal subunit at 2.4 Å resolution. *Science* 289, 905–920.
- (54) Kapust, R. B., and Waugh, D. S. (2000) Controlled intracellular processing of fusion proteins by TEV protease. *Protein Expression Purif.* 19, 312–318.
- (55) Fox, J. D., and Waugh, D. S. (2002) Maltose-binding protein as a solubility enhancer. *Methods Mol. Biol.* 205, 99–117.
- (56) Trimpin, S., Marshall, D. D., Karki, S., Madarshahian, S., Hoang, K., Meher, A. K., Pophristic, M., Richards, A. L., Lietz, C. B., Fischer, J. L., Elia, E. A., Wang, B., Pagnotti, V. S., Lutomski, C. A., El-Baba, T. J., Lu, I. C., Wager-Miller, J., Mackie, K., McEwen, C. N., and Inutan, E. D. (2020) An overview of biological applications and fundamentals of new inlet and vacuum ionization technologies. *Rapid Commun. Mass Spectrom.*, e8829.
- (57) Trimpin, S., Lutomski, C. A., El-Baba, T. J., Woodall, D. W., Foley, C. D., Manly, C. D., Wang, B., Liu, C., Harless, B. M., Kumar, R., Imperial, L. F., and Inutan, E. D. (2015) Magic matrices for ionization in mass spectrometry. *Int. J. Mass Spectrom.* 377, 532–545.
- (58) Mattiuzzo, M., De Gobba, C., Runti, G., Mardirossian, M., Bandiera, A., Gennaro, R., and Scocchi, M. (2014) Proteolytic activity of Escherichia coli oligopeptidase B against proline-rich antimicrobial peptides. *J. Microbiol. Biotechnol.* 24, 160–167.
- (59) Böttger, R., Hoffmann, R., and Knappe, D. (2017) Differential stability of therapeutic peptides with different proteolytic cleavage sites in blood, plasma and serum. *PLoS One* 12, No. e0178943.
- (60) Moazed, D., and Noller, H. F. (1987) Interaction of antibiotics with functional sites in 16S ribosomal RNA. *Nature* 327, 389–394.
- (61) Woodcock, J., Moazed, D., Cannon, M., Davies, J., and Noller, H. F. (1991) Interaction of antibiotics with A- and P-site-specific bases in 16S ribosomal RNA. *EMBO J.* 10, 3099–3103.
- (62) Lamichhane, T. N., Abeydeera, N. D., Duc, A.-C. E., Cunningham, P. R., and Chow, C. S. (2011) Selection of peptides targeting helix 31 of bacterial 16S ribosomal RNA by screening M13 phage-display libraries. *Molecules* 16, 1211–1239.
- (63) Petrov, A. S., Bernier, C. R., Hershkovits, E., Xue, Y., Waterbury, C. C., Hsiao, C., Stepanov, V. G., Gaucher, E. A., Grover, M. A., Harvey, S. C., Hud, N. V., Wartell, R. M., Fox, G. E., and Williams, L. D. (2013) Secondary structure and domain architecture of the 23S and 5S rRNAs. *Nucleic Acids Res.* 41, 7522–7535.
- (64) Bulkley, D., Innis, C. A., Blaha, G., and Steitz, T. A. (2010) Revisiting the structures of several antibiotics bound to the bacterial ribosome. *Proc. Natl. Acad. Sci. U. S. A. 107*, 17158–17163.

- (65) Schlünzen, F., Zarivach, R., Harms, J., Bashan, A., Tocilj, A., Albrecht, R., Yonath, A., and Franceschi, F. (2001) Structural basis for the interaction of antibiotics with the peptidyl transferase centre in eubacteria. *Nature* 413, 814–821.
- (66) Yonath, A. (2005) Antibiotics targeting ribosomes: resistance, selectivity, synergism and cellular regulation. *Annu. Rev. Biochem.* 74, 649–679.
- (67) Dunkle, J. A., Xiong, L., Mankin, A. S., and Cate, J. H. (2010) Structures of the Escherichia coli ribosome with antibiotics bound near the peptidyl transferase center explain spectra of drug action. *Proc. Natl. Acad. Sci. U. S. A.* 107, 17152–17157.
- (68) Sakakibara, Y., and Chow, C. S. (2011) Probing conformational states of modified helix 69 in 50S ribosomes. *J. Am. Chem. Soc.* 133, 8396–8399.
- (69) Polikanov, Y. S., Steitz, T. A., and Innis, C. A. (2014) A proton wire to couple aminoacyl-tRNA accommodation and peptide-bond formation on the ribosome. *Nat. Struct. Mol. Biol.* 21, 787–793.
- (70) Sanbonmatsu, K. Y., Joseph, S., and Tung, C.-S. (2005) Simulating movement of tRNA into the ribosome during decoding. *Proc. Natl. Acad. Sci. U. S. A. 102*, 15854–15859.
- (71) Burakovsky, D. E., Sergiev, P. V., Steblyanko, M. A., Kubarenko, A. V., Konevega, A. L., Bogdanov, A. A., Rodnina, M. V., and Dontsova, O. A. (2010) Mutations at the accommodation gate of the ribosome impair RF2-dependent translation termination. *RNA* 16, 1848–1853.
- (72) Kapust, R. B., Tözsér, J., Copeland, T. D., and Waugh, D. S. (2002) The P1' specificity of tobacco etch virus protease. *Biochem. Biophys. Res. Commun.* 294, 949—955.
- (73) Knappe, D., Ruden, S., Langanke, S., Tikkoo, T., Ritzer, J., Mikut, R., Martin, L. L., Hoffmann, R., and Hilpert, K. (2016) Optimization of oncocin for antibacterial activity using a SPOT synthesis approach: extending the pathogen spectrum to Staphylococcus aureus. *Amino Acids* 48, 269–280.
- (74) Tijerina, P., Mohr, S., and Russell, R. (2007) DMS footprinting of structured RNAs and RNA-protein complexes. *Nat. Protoc.* 2, 2608–2623.
- (75) Hulscher, R. M., Bohon, J., Rappé, M. C., Gupta, S., D'Mello, R., Sullivan, M., Ralston, C. Y., Chance, M. R., and Woodson, S. A. (2016) Probing the structure of ribosome assembly intermediates in vivo using DMS and hydroxyl radical footprinting. *Methods* 103, 49–56.
- (76) Rouskin, S., Zubradt, M., Washietl, S., Kellis, M., and Weissman, J. S. (2014) Genome-wide probing of RNA structure reveals active unfolding of mRNA structures in vivo. *Nature* 505, 701–705.
- (77) Ding, Y., Tang, Y., Kwok, C. K., Zhang, Y., Bevilacqua, P. C., and Assmann, S. M. (2014) In vivo genome-wide profiling of RNA secondary structure reveals novel regulatory features. *Nature* 505, 696–700